Ceramics-Silikáty 68 (3), 378-388 (2024)
www.ceramics-silikaty.cz doi: 10.13168/cs.2024.0037

BENEFITS OF AN ALKALINE WASHING PRE-TREAMENT OF MSWI FA BEFORE ALKALI-ACTIVATION

ZUNCHAO REN*, JUNJIE ZHANG*, LIANWANG YUAN**, #QINGSONG ZHANG*

*Geotechnical and Structural Engineering Research Center, Shandong University, Jinan, China
**Shandong Hi-speed Maintenance Group Co., LTD.

#E-mail: zhangqingsong@sdu.edu.cn

Submitted April 30, 2024; accepted June 10, 2024

Keywords: MSWI FA, Alkali washing pre-treatment, Bubbles, Heavy metals

To reveal the specific reason for the bubble release and expansion of municipal solid waste incineration fly ash (MSWI FA) during polymerisation, the chemical composition and source of the emitted gas were studied at length in this paper. To further explore the advantage of an alkali washing pre-treatment for MSWI FA, the influence and mechanism of the alkali washing pre-treatment on the macroscopic mechanical properties, microscopic pore structure and heavy metal leaching of geopolymers have been investigated. The results show that the emerging bubbles are mainly H_2 and NH_3 released by the reaction of elemental aluminium and ammonium salts from MSWI FA with alkali, respectively. The alkaline washing pre-treatment can ensure the volume stability of the geopolymers by releasing bubbles in advance, which is conducive to improving the strength of hardened paste and hindering the leaching of heavy metals. Although the alkaline washing process cannot significantly remove heavy metal ions directly, it can remove almost all the soluble chlorine salts and has a certain significance for the development of the overall compressive strength.

INTRODUCTION

With the continuous growth of urban waste, waste incineration has the advantages of saving land resources, protecting the environment and generating electricity, so it has become the mainstream method of waste disposal in recent years [1]. The latest figures show that the disposal rate of municipal solid waste in China has exceeded 99.9 %. Furthermore, incineration disposal and safe landfills account for 72.5 and 21.0 % of the total treatment, respectively. Before the year 2022, China had 583 domestic waste incineration stations, with a daily waste incineration capacity of more than one million tonnes [2]. At the same time, generating electricity from municipal solid waste, an effective and creative waste-to-energy approach, is nowadays a widely accepted technology that helps reduce the volume by 80 % and relieve any power tension [3]. As a by-product of the waste incineration power plant, municipal solid waste incineration fly ash (MSWI FA) has been labelled as hazardous waste all over the world owing to its higher content of potentially toxic heavy metals and organic pollutants [4-9]. In terms of the safe utilisation of the MSWI FA, the most concerned focus is how to ensure a lower volume expansion rate and toxic heavy metal leaching rate [10-12].

Geopolymers have attracted more and more interested scholars in recent years, largely due to saving non-renewable energy [13, 14], reducing carbon dioxide emissions [15], their excellent mechanical properties as well as having reliable durability [16-18]. At the same time, geopolymers have better toxic metal solidification/stabilisation properties than Portland cement by adsorption, physical encapsulation, chemical bonding, and so on [19-21]. These environmental benefits and unique advantages make geopolymers an ideal selection for MSWI FA. Research studies have shown that MSWI FA can realise the reuse of resources, such as mineral admixtures and precursors of geopolymers, due to the pozzolanic activity and considerable Ca and Al elements [22-24]. Al-Ghouti et al [25] showed that geopolymers prepared with MSWI FA can replace traditional cement-based materials to a certain extent. Jin [26] and Tian [27] pointed out that a small amount of MSWI FA is conducive to strength development and durability optimisation, which may be due to the introduction of active elements in MSWI FA. Lei et al. [28] successfully prepared a product with a strength of over 21 MPa at 7 d by reacting pure MSWI FA with a complex alkali solution. Zheng et al [29] and Wongsa et al. [30] prepared products with a strength of 73.57 and 53.0 MPa for 28 d using MSWI FA, respectively. MSWI FA has shown to have remarkable potential for its base-stimulating activity.

Some experimental studies have found that the pre-treatment of MSWI FA before alkali activation can particularly reduce the toxic metal leaching rate [31]. Lin et al. [32] enhanced the ability of MSWI FA

to fix Cr by ultrasonic-assisted washing. Chen et al. [33] found that the mechanical activation of MSWI FA could improve the strength of the material and reduce the leaching of toxic metals by adjusting the amount of nitric acid and sodium carbonate. Dontriros et al. [34] removed chloride ions and sulfate ions, and effectively inhibited the leaching of toxic metals. Zheng et al. [29] explained that a water-wash can remove almost all the NaCl and KCl, improving the degree of polymerisation of the geopolymer, as well as reducing the toxic metal leaching. However, the above studies cannot solve the problem of volume expansion caused by the gas formation of MSWI FA in an alkaline environment. Although few articles have mentioned that an alkaline washing pre-treatment may prevent the occurrence of volume expansion, the cause and mechanism of the expansion are still unclear. At the same time, the pungent odour associated with the occurrence of the gas is clearly not caused by the elemental aluminium alone, and there is no relevant research on its source.

Therefore, starting from the generated gas, this paper explores the chemical composition and source of the gas. In addition, the effect of the released gas on the pore structure of the hardened slurry is explained. Combined with the removal effect of soluble chlorine salts, the advantages and mechanism of the alkaline washing pre-treatment are comprehensively explained. Finally, it is sincerely hoped that the reasonable resource utilisation of MSWI FA can be a contribution of this paper.

EXPERIMENTAL

Materials

MSWI FA

All the MSWI FA in this work was produced from mechanical grate furnaces and provided by the Waste Incineration Power Plant of China Everbright Group. It is important to note that the MSWI FA is taken directly from the bottom of the chimney and has not been treated with chelating agents. The elementary composition and particle distribution of MSWI FA can be seen in Table 1 and Figure 1a respectively.

GBFS, Steel, and Fly ash

The GBFS, steel, and fly ash are provided by Shandong Jingnuo Building Materials Co., Ltd., China, and their chemical composition and particle distribution can be seen in Table 1 and Figure 1b, c, d respectively.

Na_2SiO_3

The Na_2SiO_3 was provided by Suzhou Youchuang Chemical Environmental Protection Technology Co., Ltd, China, and its modulus is 2.4 in this work.

Methods

Alkaline washing pre-treatment

To systematically demonstrate the influence of the alkaline wash pre-treatment on the ingredients in the MSWI FA, a set of specific experimental procedures were used that can be seen in Figure 2. Prior to the experiment, 100 g of MSWI FA was put into conical bottles. By adjusting the amount of the alkali control water, the solid ratio and pH were adjusted to 5:1 and 9, respectively. The upward exhaust air method was used to collect the gas substances generated in the experiment, and then a gas chromatography-mass spectrometer (GC–MS) was used for the gas composition analysis. The MSWI FA in the conical bottles was collected and analysed by an X-ray diffractometer (XRD), an organic composition analyser, and a Fourier transform infrared spectrometer (FT-IR).

SP analysis

Spectrophotometry (SP) was used to detect the NH_4^+ in the MSWI FA washing solution. To conduct the experiment, different volumes of an ammonium standard solution (0.01 $mg{\cdot}mL^{-1}$) were absorbed into a 50 ml colorimetric tube, namely 0, 0.5, 1.0, 3.0, 5.0, 7.0, and 10.0 mL. Then, 1 mL of potassium sodium tartrate ($KNaC_4H_4O_6{\cdot}4H_2O$) and 1.5 mL of a sodium reagent (containing NaOH, KI, and HgI_2) were added to the tube, followed by dilution with water up to the marked line. Using a wavelength of 430 nm and a path length of 10 mm, the absorbance of each solution was measured, and a standard curve was plotted. Likewise, drops of the MSWI FA washing liquid were

Table 1. Chemical compositions of the raw materials (wt. %).

	SiO_2	Al_2O_3	Fe_2O_3	CaO	MgO	K_2O	Na_2O	SO_3	Cl	Others
MSWI FA	5.75	4.49	6.32	35.26	1.02	7.57	0.67	7.36	28.24	3.32
GBFS	28.6	14.3	4.68	38	9.36	0	0	1.76	0.02	3.28
Steel slag	14.09	5.03	19	45.19	6.53	0.04	0.11	1.21	0.03	8.77
Fly ash	48.5	26.8	3.89	8.72	0.98	1.1	0	1.72	0.03	8.25

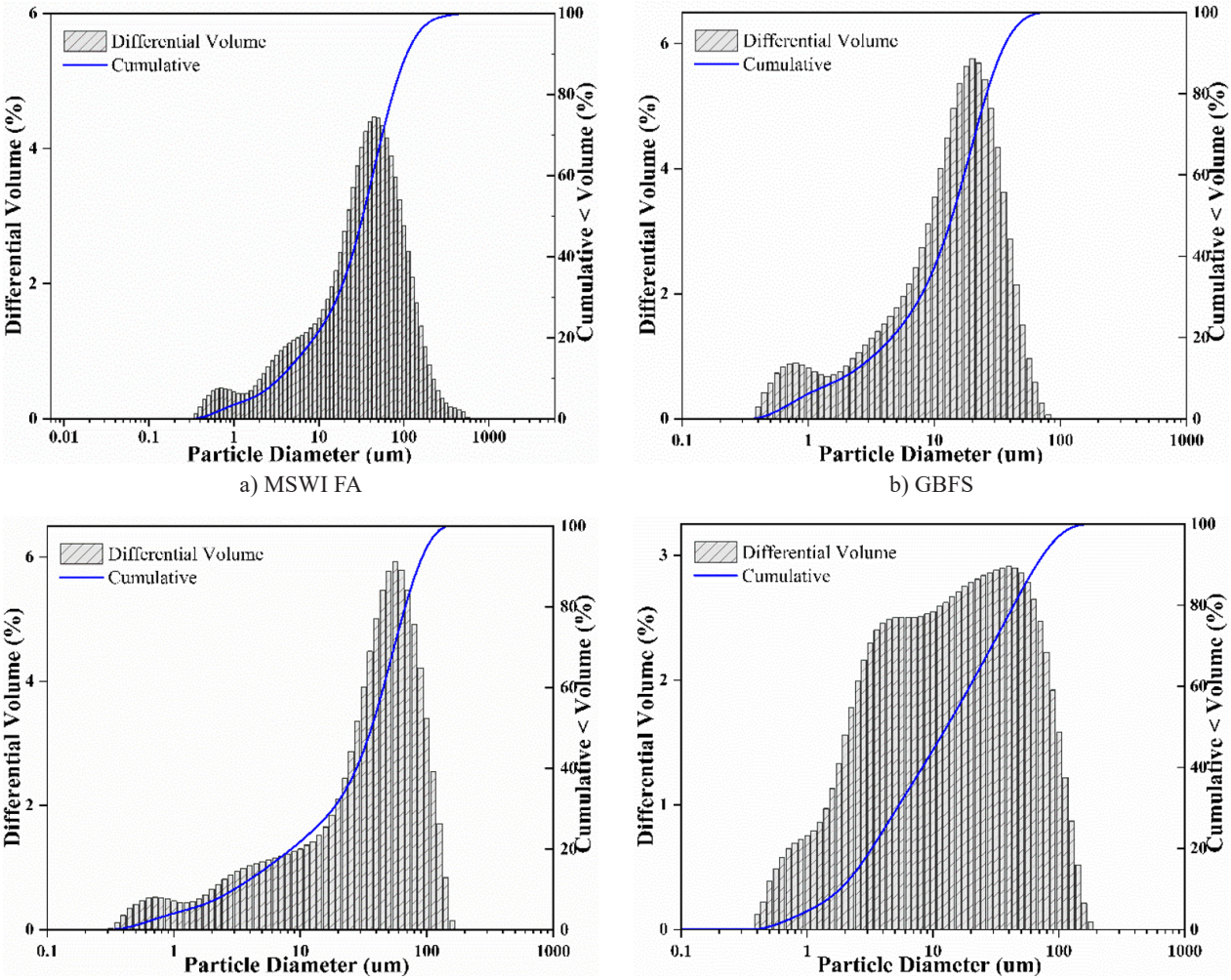

a) MSWI FA b) GBFS

c) Steel slag d) Fly ash

Figure 1. Particle distribution of the raw materials.

added to a 50 ml colorimetric tube, along with 1 mL of potassium sodium tartrate and 1.5 mL of the sodium reagent. The absorbance of these samples was measured, and the NH_4^+ content was determined by comparing it with the values obtained from the standard curve.

XRD analysis

The XRD patterns were obtained with an X-ray diffractometer (D8-Advance) made by Bruker in Germany. With this instrument, the consistent test rate was set to 4 °·min^{-1}, ranging between 10° and 90°, in steps of 0.05°.

XRF and ICP-MS analysis

The XRF and ICP-MS were obtained using an X-ray fluorescence spectrometer (S2 PUMA Series II) and an Inductive Coupled Plasma Emission Spectrometer (Elan DRC-e, PerkinElmer), respectively.

FT-IR analysis

An FT-IR analyser (Thermo Fisher, Nicolet iS5, USA) was used for the raw MSWI FA and pre--treated MSWI FA. In this experiment, the test range of the sample was from 400 to 4000 cm^{-1}.

Preparation and curing of the samples

All the raw materials are made from the same batch and were processed in a room at 20 ± 2 ℃. A Na_2SiO_3 powder was used for the alkali-active substance, with the water-binder ratio being controlled to 0.45. The specific experimental mix can be seen in Table 2. Among the mixes, the MSWI FA used in FA-2, 4, 6, and 8 were pre-treated by alkali washing. Six samples with dimensions of 40 × 40 × 160 mm were prepared with each ratio and placed in a standard curing box (25 ± 2 ℃, greater than 95 % humidity) until the next test was performed.

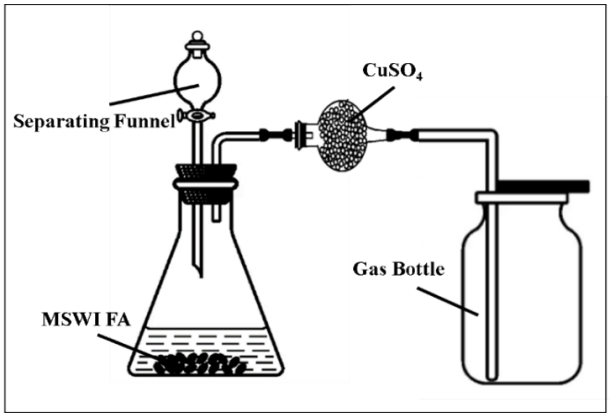

Figure 2. Experimental diagram of the alkaline washing pre--treatment.

Compressive strength test

The uniaxial unconfined compressive strength of the geopolymer was collected by a universal testing machine (MTS, CMT5504, 100 KN). All the geopolymer samples were placed on the test bench in turn, with a loading speed of $5N{\cdot}s^{-1}$ selected. Six samples of each group were measured and their average value was taken as the final result.

Pore structure analysis

The pore structure analysis was performed by a low field NMR instrument (MacroMR12-150V-I). For the measuring accuracy of the results, the sample should cbe strictly maintained at 25 °C all the while. With the sampling frequency set to 250 kHz, 4000 echoes were recorded and the time of each echo was 0.4 ms.

Heavy metal analysis

The collection process of heavy metal ions was performed through the strong acid digestion method and the HJT300-2007 standard leaching test, respectively. The detection process was determined by inductively coupled plasma optical emission spectrometry (ICP-OES; Prodigy XP, Leeman-Labs).

RESULTS AND DISCUSSION

Results of the alkaline washing pre-treatment

Gas phase analysis

In the process of preparing the hardened paste by MSWI FA and the alkali solution, a large number of bubbles will be produced, resulting in the volume expansion of the paste and accompanying pungent odour. To collect as pure a sample as possible, the gas collection time is limited to the first two hours with the fastest generation rate [35]. The gases collected from the device were imported into the GC-MS for the gas composition analysis, and the analysis results are shown in Table 2. It is obvious that H_2 is the main product of all the formed gases, with a content of 85.7 %. Considering the chemical composition of the MSWI FA, only the elemental aluminium can react with the alkali solution to produce H_2. The elemental aluminium remains protected by a thin film of alumina, which explains the source of the H_2, and the reaction equation that is shown in (1).

Table 2. Gas composition from the GC-MS.

Gas	Hydrogen	Propane	Pentane	Others	Unknown
Proportion	85.7 %	2.1 %	0.8 %	2.9 %	8.5 %

$$2Al + 2OH^- + 2H_2O \rightarrow 2AlO_2^- + 3H_2 \quad (1)$$

$$NH_4^+ + OH^- \rightarrow NH_3 + H_2O \quad (2)$$

H_2 can also explain the MSWI FA expansion reaction with the alkali solution, but still cannot explain the pungent odour source. Therefore, it is reasonable to assume that there may be another gas that has not been detected because the concentration is too low to meet the detection limit of the GC-MS. The sample (before and after the alkali wash pre-treatment) is completely burned in the oxidation tube at 1150 ℃ in a pure oxygen atmosphere to produce CO_2, H_2O, NO_x, SO_2, SO_3 and other gases, and then the mixture is further reduced into CO_2, H_2O, N_2, SO_2 and other gases in the reduction tube (850 ℃, reduced copper). After separation by the adsorption-desorption column, the thermal conductivity detection after separation was carried out through a chromatographic column. The contents of the C, H, N and S elements were obtained, and the results are shown in Table 3. This result shows that the alkaline washing pre-treatment reduced the N and S elements in the MSWI FA by 1.23 and 0.54 %, respectively. NH_3, SO_2 and SO_3 all give off pungent odours. NH_3 is the product of the reaction of the alkali solution with the ammonium salt in MSWI FA, as in Equation (2), while SO_2 and SO_3 are derived from the attachments during the high-temperature formation of MSWI FA.

Table 3. Organic element analysis.

Sample	N (%)	C (%)	H (%)	S (%)
Before alkali wash pre-treatment	1.45	3.03	2.11	3.09
After alkali wash pre-treatment	0.22	4.93	1.25	2.55

To further prove the existence of the ammonium salt in MSWI FA, NH_4^+ was detected by a spectrophotometer. Figure 3 shows the determination results. The standard

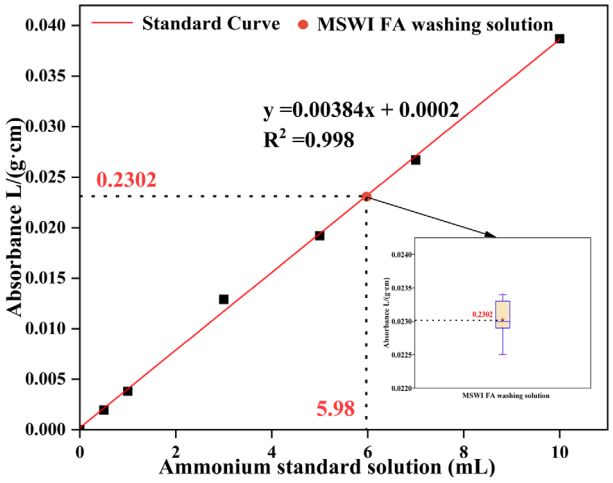

Figure 3. Absorbance at 430 nm.

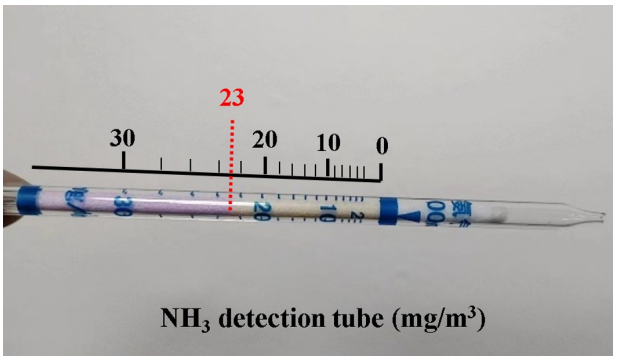

Figure 4. NH_3 detection tube.

curve is prepared from a 0, 0.5, 1.0, 3.0, 5.0, 7.0 and 10.0 mL ammonium standard solution (0.01 mg·mL^{-1}) diluted to 50 mL. By comparing the absorbance measured by the 50 mL MSWI FA washing solution (water solid ratio is 5:1) with the standard curve, the mass of NH_4^+ can be obtained, and then the concentration of the ammonium salt in the washing solution can be calculated as 1.2 ppm. The presence of NH_4^+ in the washing solution provides the possibility for the formation of NH_3 in the alkaline washing process. On the other hand, the NH_3 detection tube (Figure 4) was used to measure 23 mg·m^{-3} in the sample gas through the principle of the linear colorimetric method, which further confirmed that NH_3 could be released by the reaction of MSWI FA with the alkali solution.

XRD analysis

The collected XRD information of MSWI FA is shown in Figure 5. Chlorine salts (NaCl, KCl, and CaClOH) and calcium salts ($CaCO_3$, $CaSO_4$, and $Ca(Al, Si)_2O_4$) are the dominant state of existence in MSWI FA [36], which corresponds to the results of the previous elemental analysis. Specifically,

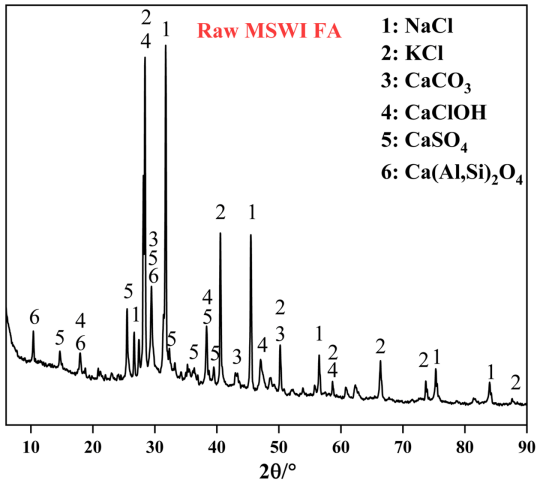

a) Raw MSWI FA

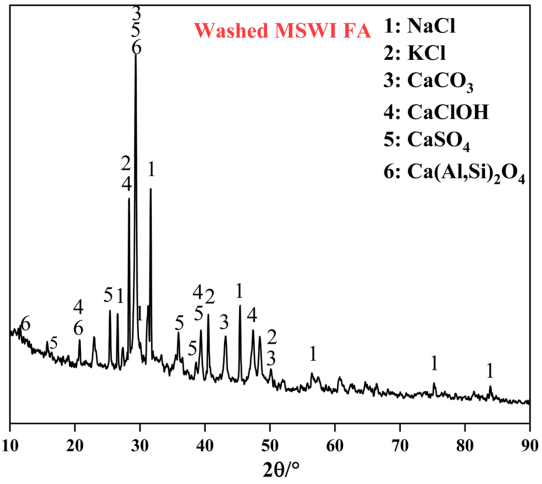

b) Washed MSWI FA

Figure 5. XRD patterns of the MSWI FA, the left picture is the raw MSWI FA and the right picture is the washed MSWI FA.

the chlorine elements mostly existed in the forms of soluble chloride such as NaCl, KCl, and CaClOH, and their content decreased significantly after the alkaline washing pre-treatment. It is worth noting that cal-cium salts contribute to the formation of products and the improvement of the properties in the cementitious material system. Whether MSWI FA is used for solidified landfills or recycled resources, calcium salts can play a certain contribution [37]. The decrease in the chlorine content leads to an increase in the calcium content, so MSWI FA can play a better role in the cementitious material system after the alkali washing pre-treatment, which is consistent with the previous conclusions [38].

XRF and ICP-MS analysis

Comparing the elemental changes in the raw and the washed MSWI FA, it can be observed that the percentage content of the Cl significantly decreases,

Table 4. Elemental composition of the MSWI FA (%).

Content	Ca	Cl	K	Na	Si	Al	Fe	Mg	S	Others
Raw	44.125	21.064	6.988	4.078	4.173	1.606	3.397	3.032	9.003	2.264
Washed	52.901	7.871	3.06	2.406	7.44	2.651	4.804	4.585	11.307	3.056

Table 5. Heavy metals of the MSWI FA (mg·kg^{-1}).

Total	Pb	Zn	Cu	Cd	Cr	Ba	Ni
Raw	1424.38	2343.13	675.87	108.77	90.74	627.15	60.36
Washed	1259.13	2267.44	659.93	112.55	113.75	660.59	56.18

while the content of K and Na also decreases to varying degrees. On the other hand, the content of the other elements, such as Ca, Si, and Al, increases. This can be attributed to the alkali washing pre-treatment process, which effectively removes a large portion of chloride salts and results in the enrichment of Ca, as shown in Table 4. However, the alkaline washing process is not effective in removing heavy metal ions other than Pb, as shown in Table 5, which may be due to the high solubility of Pb in water.

FT-IR analysis

The FTIR analysis is helpful for an in-depth analysis of the molecular structure and chemical bonds between the atoms of the MSWI FA. Figure 6 shows the chemical state of the MSWI FA (raw or washed), which is mainly composed of six absorption peaks. The narrow absorption peak at 875 cm^{-1} corresponds to the symmetrical stretching vibration of O-C-O [39], which corresponds to the presence of $CaCO_3$ in Figure 4. The peak at 970 cm^{-1} is represented by the tensile vibration of the Si-O-Si bond in the silicate [40], corresponding to the $Ca(Al,Si)_2O_4$ mineral in the XRD analysis. The wide absorption peak at 1124 cm^{-1} is related to the asymmetric stretching vibration of S-O [41], which is related to the presence of SO_4^{2-}. The absorption band of 1437 cm^{-1} is related to the asymmetric stretching motion of the O-C-O bond in the CO_3^{2-} [42]. The absorption peak at 1637 cm^{-1} is related to the bending vibration of the H-O-H in the bound water. Finally, the wide absorption peak at 3439 cm^{-1} is attributed to the stretching vibration of the Al-OH bond in the $[Al(OH)_6]^{3-}$ octahedral structure [43]. The washed MSWI FA has a higher peak at 3439 cm^{-1}, further proving that more elemental aluminium was involved in the reaction with the alkali solution, as shown in Equation (1) and (3).

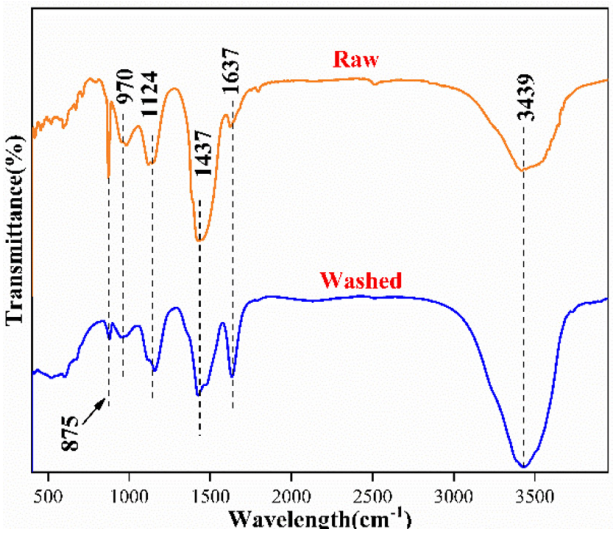

Figure 6. FTIR of the MSWI fly ash.

$$AlO_2^- + 2OH^- + 2H_2O \rightarrow [Al(OH)_6]^{3-} \qquad (3)$$

Compressive strength analysis

To investigate the improvement effect of the alkaline washing pre-treatment on the macroscopic performance of the MSWI FA, the washed MSWI FA was tested for its compressive strength. Different mix ratios were designed with MSWI FA, GBFS, steel slag, and fly ash, as illustrated in Table 6.

Table 6. The mix ratio of the experimental samples (g).

	MSWI FA	GBFS	Steel slag	Fly ash	Water	Na_2SiO_3
FA-1	200	0	0	0	90	14
FA-2	200	0	0	0	90	14
FA-3	80	120	0	0	90	14
FA-4	80	120	0	0	90	14
FA-5	60	0	140	0	90	14
FA-6	60	0	140	0	90	14
FA-7	60	0	0	140	90	14
FA-8	60	0	0	140	90	14

Note: The MSWI FA used in FA-2, FA-4, FA-6 and FA-8 is washed with alkali

The compressive strength of the samples with the different proportions and different curing ages is shown in Figure 7. FA-1 and FA-2 are the samples prepared from pure MSWI FA, and FA-2 1obviously has higher strength than FA-in each age after the alkaline washing pre-treatment, which indicates that the removal

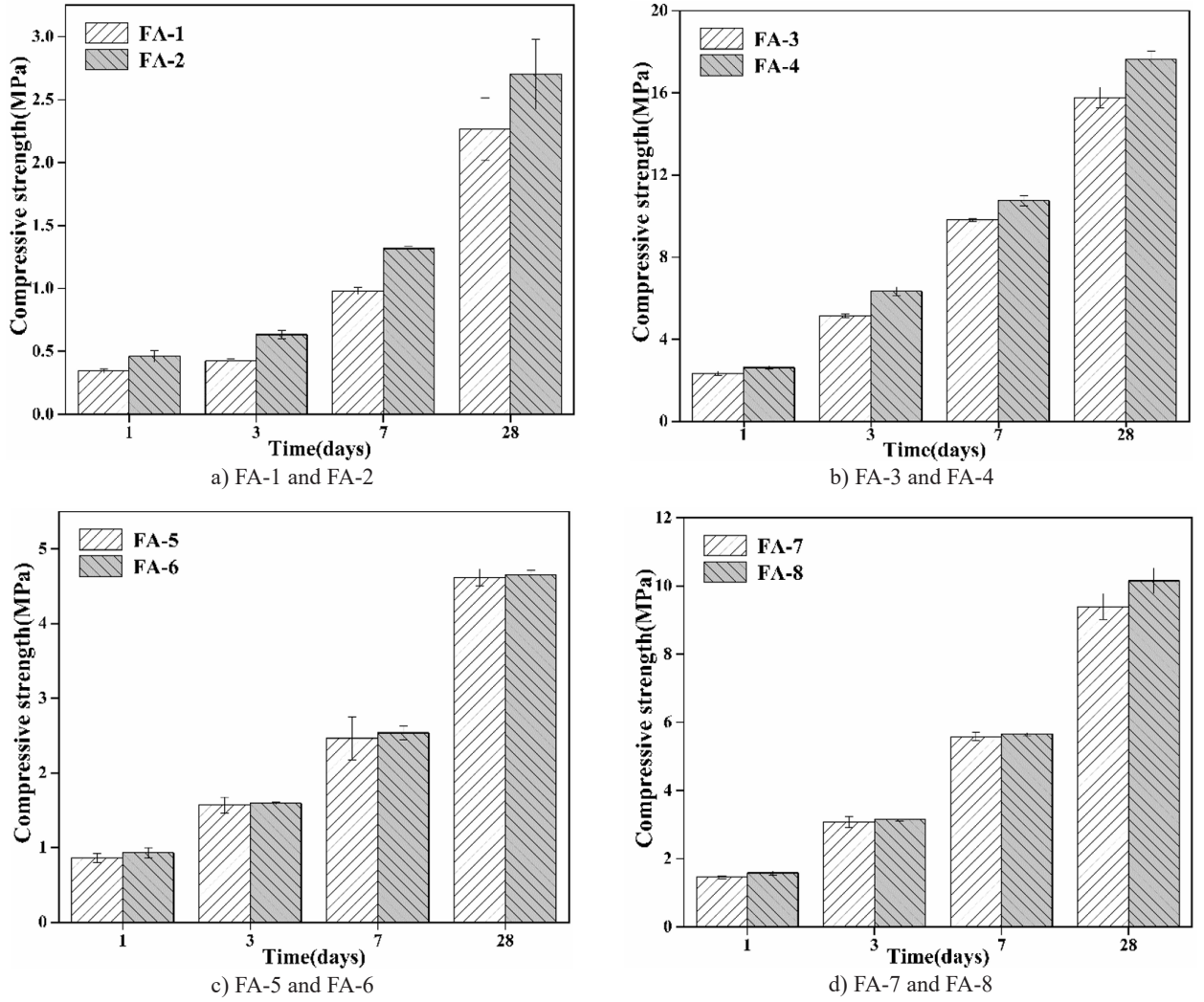

Figure 7. Compressive properties.

of the gas and soluble chlorine salts by alkaline washing pre-treatment is very beneficial to the development of the strength. It is the pure MSWI FA prepared samples that have relatively lower strength, whose strength at 1 and 28 d do not exceed 0.5 and 3 MPa, respectively. FA-3 and FA-4 have significantly higher strength, and the strength at 28 d can reach more than 16 MPa, which shows that MSWI FA still has some value to partially replace the cementitious material and can be reused as a resource. The combination of MSWI FA and steel slag (FA-5 and FA-6) has no outstanding performance, whose strength at 1 and 28 d is less than 1 and 5 MPa, respectively, because the MSWI FA and steel slag are rich in Ca elements, but lack Si and Al elements that provide any skeletal support in the cementing system [44]. The strength of FA-7 and FA-8 at 28 d can reach about 10 MPa, which is closely related to the action of the fly ash. Although the strength difference between the different proportions was obvious, the alkaline washing pre-treatment under the same proportion of each group is always beneficial to improve the strength. This is due to the fact that alkaline washing pre-treatment can remove, in advance, the ammonium salts and elemental aluminium that produce the expansive gases as well as soluble chlorine salts that are not beneficial to the strength development.

Pore structure analysis

The low-frequency NMR can describe the pore structure of the sample qualitatively, as shown in Figure 8. Two obvious peaks can be found in each sample, where the higher and lower peaks represent the distribution of small holes from 1 to 100 nm, and the distribution of holes from 100 to 10000 nm in the sample, respectively. It can be seen that the number of small wells of the sample under the same ratio after the alkaline washing treatment decreases sharply, and the number of large wells also decreases overall. Undoubtedly, the pore structure of the sample made by the pure MSWI FA changed most obviously after the alkaline washing pre-treatment.

For the further quantitative description and in-depth exploration of the pore structure, it is necessary

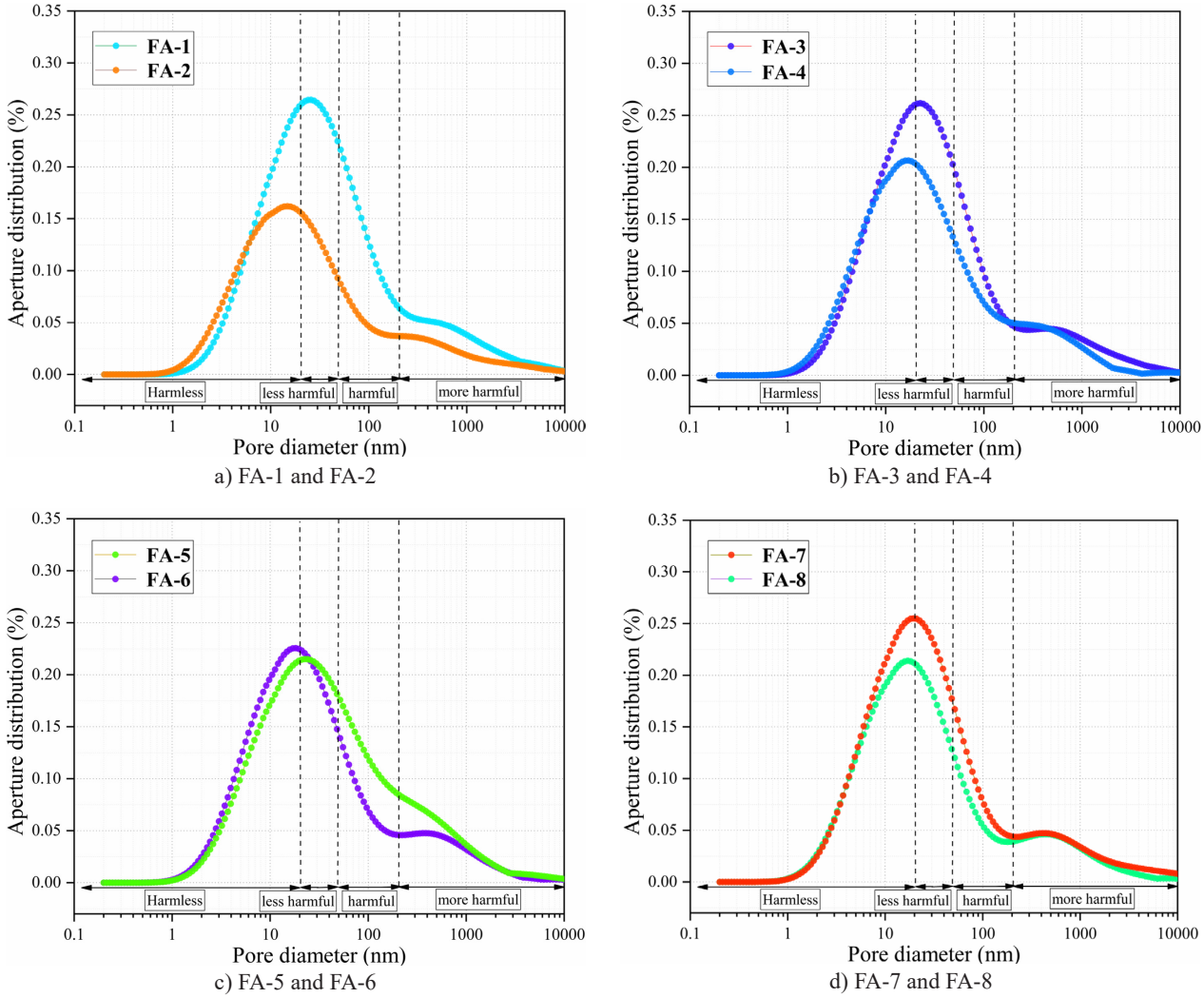

Figure 8. Pore distribution of the different samples.

to classify the pore types according to the degree of damage to the structure. Specifically, that is the porosity range corresponding to the sample from 0 to 20 nm, 20 – 50 nm, 50 – 200 nm, and above 2000 nm are considered harmless pores, less harmful pores, harmful pores, and multi-hazard pores [45]. Figure 9 shows the comparison of the classification porosity under different experimental proportions. Not only the change in the total porosity under each ratio is clear at a glance (FA-1→FA-2: 12.35→7.83; FA-3→FA-4: 11.77→9.75; FA-5→FA-6: 11.35→10.36; FA-7→FA-8: 11.64→9.78;), but also the change in the number of various types of pores is very obvious.

It is not difficult to see that the number of multi-hazard pores and harmful pores has decreased significantly, and the number of harmless pores has decreased slightly, while the number of harmless pores has not changed significantly. It can be inferred that the bubbles of the elemental aluminium and ammonium salts in the MSWI FA react with the alkali solution are mostly multi-hazard pores and harmful pores, which also explains the main reason for the increase in the strength under the same ratio after the alkali washing pre-treatment from the perspective of the microstructure.

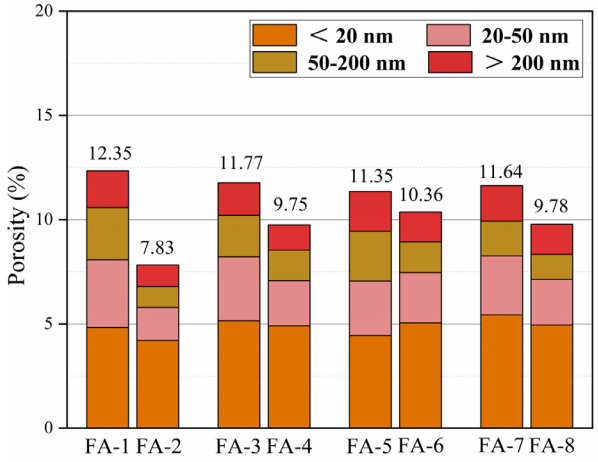

Figure 9. Comparison of the classification porosity under the different experimental proportions.

Heavy metal analysis

Figure 10 and Figure 11 show the total concentration and leaching concentration of the heavy metals under the different experimental ratios in Table 4, respectively. It can be clearly seen from Figure 10 that the concentration of various heavy metals is positively correlated with the amount of MSWI FA in the mix ratio. Almost all the samples have a high concentration of these targeted metals, and their total concentration follows the order of Zn > Pb > Ba > Cu >> Mn > Cd > Cr > Ni. The reason why the concentration of heavy metals represented by Zn do not decrease, but increased slightly after the alkaline washing pre-treatment with the same proportion is that the alkaline washing process takes away a large amount of soluble chlorine salts and indirectly increased the total concentration of the heavy metals, which is consistent with the conclusion of the XRD analysis.

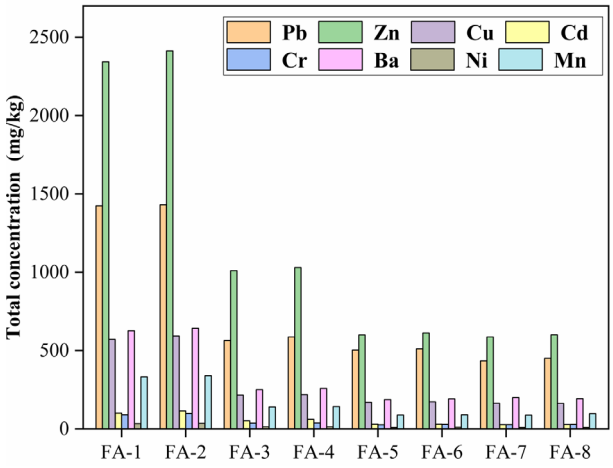

Figure 10. Total concentration of heavy metals.

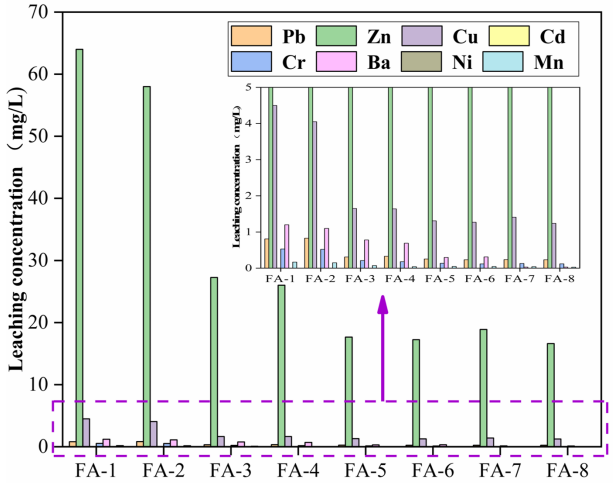

Figure 11. Leaching concentration of the heavy metals.

As shown in Figure 11, with the exception of the heavy metal Zn, only a few other heavy metals are leached. Cd and Ni are almost non-leached, which is because they are inherently less abundant than the other heavy metals. After the alkaline washing pre-treatment, the leaching concentration of all the heavy metal ions decreased overall. This phenomenon can be explained by the pore structure (Wang et al., 2022). In the process of alkali washing, a large amount of gas is released in advance to ensure the structure density of the hardened slurry and inhibit the leakage of the heavy metal ions. It is further proved that the alkaline washing pre--treatment can reduce the leaching of heavy metals. From the point of view of heavy metals, the alkali washing pre-treatment is beneficial to MSWI FA, no matter the landfill treatment or resource utilisation.

CONCLUSIONS

This paper mainly studied the optimisation of alkaline washing MSWI FA for the preparation of geopolymers. According to the test results, the following conclusions have been established:

1. The inherent elemental aluminium and ammonium salt in the MSWI FA are the main factors affecting the gas formation and volume instability. The elemental aluminium and ammonium salt will produce H_2 and NH_3, respectively, in an alkaline environment, resulting in the constant expansion of the slurry in the hardening process and destruction of the structural stability.
2. The alkaline washing pre-treatment can release the gas produced in the MSWI FA in advance, ensure the structural stability of the hardened slurry, and help to prevent the leaching process of heavy metals.
3. The alkaline washing pre-treatment can also wash away the soluble chlorine salts which do not contribute to the reactivity, which is beneficial to improve the mechanical properties of the geopolymers prepared by the MSWI FA.
4. Although the alkaline washing pre-treatment will not reduce the total concentration of the heavy metals in the MSWI FA, it can prevent the leaching behaviour of the heavy metals by improving the pore structure. Therefore, the alkaline washing pre-treatment process is beneficial for both the safe landfill and the recycling of MSWI FA.

REFERENCES

1. Song M., Lan T., Meng Y., Ju T., Chen Z., et al. (2022): Effect of microbially induced calcium carbonate precipitation treatment on the solidification and stabilization of municipal solid waste incineration fly ash (MSWI FA)-Based materials incorporated with metakaolin. *Chemosphere, 308*, 136089.

doi: 10.1016/j.chemosphere.2022.136089
2. China NBS (2022). *China Statistical Yearbook of 2022*. Chinese Statistical Bureau. China Statistical Press, Beijing.
3. Tang P., Brouwers H.J.H. (2017): Integral recycling of municipal solid waste incineration (MSWI) bottom ash fines (0–2 mm) and industrial powder wastes by cold-bonding pelletization. *Waste Management, 62*, 125-138. doi: 10.1016/j.wasman.2017.02.028
4. Huang T., Liu L., Zhou L., Yang K. (2018): Operating optimization for the heavy metal removal from the municipal solid waste incineration fly ashes in the three-dimensional electrokinetics. *Chemosphere, 204*, 294-302. doi: 10.1016/j.chemosphere.2018.04.065
5. Li W., Sun Y., Huang Y., Shimaoka T., Wang H., et al. (2019): Evaluation of chemical speciation and environmental risk levels of heavy metals during varied acid corrosion conditions for raw and solidified/stabilized MSWI fly ash. *Waste management, 87*, 407-416. doi: 10.1504/IJSTM.2019.101895
6. Li Y., Min X., Ke Y., Liu D., Tang C. (2019): Preparation of red mud-based geopolymer materials from MSWI fly ash and red mud by mechanical activation. *Waste Management, 83*, 202-208. doi: 10.1016/j.wasman.2018.11.019
7. Bai M., Zhang L., Zhao Y., Sun S., Du S., et al. (2023): Numerical simulation on the deposition characteristics of MSWI fly ash particles in a cyclone furnace. *Waste Management, 161*, 203-212. doi: 10.1016/j.wasman.2023.03.004
8. Xu T., Wu H., Jiang D., Qi N., Gou Z. (2023): Municipal solid waste incineration (MSWI) fly ash could be used as a catalyst for pyrolysis of oil-based drill cuttings from shale gas exploitation industry. *Journal of Cleaner Production, 38*7, 135754. doi: 10.1016/j.jclepro.2022.135754
9. Li T., Wang B. (2023): Effect and mechanism of nano-alumina on early hydration properties and heavy metals solidification/stabilization of alkali-activated MSWI fly ash solidified body. *Journal of Hazardous Materials, 452*, 131327. doi: 10.1016/j.jhazmat.2023.131327
10. Zheng L., Wang W., Gao X. (2016): Solidification and immobilization of MSWI fly ash through aluminate geopolymerization: based on partial charge model analysis. *Waste Management, 58*, 270-279. doi: 10.1016/j.wasman.2016.08.019
11. Su L., Fu G., Liang B., Sun Q., Zhang,X., Shen Z. (2022): Working performance and microscopic mechanistic analyses of municipal solid waste incineration (MSWI) fly ash-based self-foaming filling materials. *Construction and Building Materials, 361*, 129647. doi: 10.1016/j.conbuildmat.2022.129647
12. Li Y., Feng D., Bai C., Sun S., Zhang Y., et al. (2022): Thermal synergistic treatment of municipal solid waste incineration (MSWI) fly ash and fluxing agent in specific situation: Melting characteristics, leaching characteristics of heavy metals. *Fuel Processing Technology, 233*, 107311. doi: 10.1016/j.fuproc.2022.107311
13. Zhang Y., Liu H., Ma T., Gu G., Chen C., Hu J. (2023): Understanding the changes in engineering behaviors and microstructure of FA-GBFS based geopolymer paste with addition of silica fume. *Journal of Building Engineering, 70*, 106450. doi: 10.1016/j.jobe.2023.106450
14. Zhang M., He M., Zhang J. (2023): Mitigation of efflorescence for multi-componential geopolymer: Influence of steel slag, flue gas desulfurization gypsum and pre-curing periods. *Journal of Cleaner Production, 403*, 136835. doi: 10.1016/j.jclepro.2023.136835
15. Xiong G., Guo X., Zhang H. (2023): Preparation of epoxy resin-geopolymer (ERG) for repairing and the microstructures of the new-to-old interface. *Composites Part B: Engineering, 259*, 110731. doi: 10.1016/j.compositesb.2023.110731
16. Tang Z. Q., Sui H., de Souza F.B., Sagoe-Crentsil K., Duan W. (2023): Silane-modified graphene oxide in geopolymer: Reaction kinetics, microstructure, and mechanical performance. *Cement and Concrete Composites, 139*, 104997. doi: 10.1016/j.cemconcomp.2023.104997
17. Gill P., Jangra P., Roychand R., Saberian M., Li J. (2023): Effects of various additives on the crumb rubber integrated geopolymer concrete. *Cleaner Materials, 8*, 100181. doi: 10.1016/j.clema.2023.100181
18. Sun B., Sun Y., Ye G., De Schutter G. (2022): A mix design methodology of slag and fly ash-based alkali-activated paste. *Cement and Concrete Composites, 126*, 104368. doi: 10.1016/j.cemconcomp.2021.104368
19. Muhammad F., Huang X., Li S., Xia M., Zhang M., et al. (2018): Strength evaluation by using polycarboxylate superplasticizer and solidification efficiency of Cr^{6+}, Pb^{2+} and Cd^{2+} in composite based geopolymer. *Journal of cleaner production, 188*, 807-815. doi: 10.1016/j.jclepro.2018.04.033
20. Lancellotti I., Barbieri L., Leonelli C. (2015). Use of alkali-activated concrete binders for toxic waste immobilization. In *Handbook of alkali-activated cements, mortars and concretes* (pp. 539-554). Woodhead Publishing. doi: 10.1533/9781782422884.4.539
21. Fan X., Zhou Z., Huang B., Ji Z., Gan M., et al. (2022): Mineralization behavior and strengthening technology of high calcium MSWI fly ash in sintering co-treatment process. *Journal of Materials Research and Technology, 20*, 1127-1141. doi: 10.1016/j.jmrt.2022.07.118
22. Ferone C., Colangelo F., Messina F., Santoro L., Cioffi R. (2013): Recycling of pre-washed municipal solid waste incinerator fly ash in the manufacturing of low temperature setting geopolymer materials. *Materials, 6*(8), 3420-3437. doi: 10.3390/ma6083420
23. Long L., Zhao Y., Lv G., Duan Y., Liu X., Jiang X. (2023): Improving stabilization/solidification of MSWI fly ash with coal gangue based geopolymer via increasing active calcium content. *Science of the Total Environment, 854*, 158594. doi:10.1016/j.scitotenv.2022.158594
24. Fan C., Wang B., Qi Y., Liu Z. (2021): Characteristics and leaching behavior of MSWI fly ash in novel solidification/stabilization binders. *Waste Management, 131*, 277-285. doi: 10.1016/j.wasman.2021.06.011
25. Al-Ghouti M. A., Khan M., Nasser M.S., Al-Saad K., Heng O.E. (2021): Recent advances and applications of municipal solid wastes bottom and fly ashes: Insights into sustainable management and conservation of resources. Environmental Technology & Innovation, 21, 101267. doi:10.1016/j.eti.2020.101267
26. Jin M., Zheng Z., Sun Y., Chen L., Jin Z. (2016): Resistance of metakaolin-MSWI fly ash based geopolymer to acid and alkaline environments. *Journal of Non-Crystalline Solids, 450*, 116-122. doi:10.1016/j.jnoncrysol.2016.07.036
27. Tian X., Rao F., León-Patiño C.A., Song S. (2021): Co-disposal of MSWI fly ash and spent caustic through alkaline-activation consolidation. *Cement and Concrete Composites,*

116, 103888. doi: 10.1016/j.cemconcomp.2020.103888
28. Zheng L., Wang W., Shi Y. (2010): The effects of alkaline dosage and Si/Al ratio on the immobilization of heavy metals in municipal solid waste incineration fly ash-based geopolymer. *Chemosphere, 79*(6), 665-671. doi: 10.1016/j.chemosphere.2010.02.018
29. Zheng L., Wang C., Wang W., Shi Y., Gao X. (2011): Immobilization of MSWI fly ash through geopolymerization: effects of water-wash. *Waste Management, 31*(2), 311-317. doi: 10.1016/j.wasman.2010.05.015
30. Wongsa A., Boonserm K., Waisurasingha C., Sata V., Chindaprasirt P. (2017): Use of municipal solid waste incinerator (MSWI) bottom ash in high calcium fly ash geopolymer matrix. *Journal of Cleaner Production, 148*, 49-59. doi:10.1016/j.jclepro.2017.01.147
31. Righi C., Lancellotti I., Barbieri L., Kirkelund G.M. (2022): Benefits of pre-treating MSWI fly ash before alkali-activation. *Sustainable Chemistry and Pharmacy, 27*, 100671. doi: 10.1016/j.scp.2022.100671
32. Lin S., Lu Y., Zheng L., Long L., Jiang X., Yan J. (2023): Immobilization potential of Cr through Ultrasonic-assisted water washing in MSWI fly ash and evaluation of carbon capture and product reuse in its washing liquid. *Process Safety and Environmental Protection, 174*, 627-636. doi: 10.1016/j.psep.2023.04.035
33. Chen Z., Lu S., Tang M., Ding J., Buekens A., et al. (2019): Mechanical activation of fly ash from MSWI for utilization in cementitious materials. *Waste Management, 88*, 182-190. doi: 10.1016/j.wasman.2019.03.045
34. Dontriros S., Likitlersuang S., Janjaroen D. (2020): Mechanisms of chloride and sulfate removal from municipal-solid-waste-incineration fly ash (MSWI FA): Effect of acid-base solutions. *Waste Management, 101*, 44-53. doi: 10.1016/j.wasman.2019.09.033
35. Huang G., Yang K., Chen L., Lu Z., Sun Y., et al. (2020): Use of pretreatment to prevent expansion and foaming in high-performance MSWI bottom ash alkali-activated mortars. *Construction and Building Materials, 245*, 118471. doi: 10.1016/j.conbuildmat.2020.118471
36. Fan C., Wang B., Ai H., Liu Z. (2022): A comparative study on characteristics and leaching toxicity of fluidized bed and grate furnace MSWI fly ash. *Journal of environmental management, 305*, 114345. doi: 10.1016/j.jenvman.2021.114345
37. Zhang C., Yang J., Chen Z., Gong H., Zhao Z., Zhang H. (2023): Reuse of waste sulfur from biogas desulfurization for potentially toxic metals stabilization in MSWI fly ash towards zero-waste in venous industry park. *Journal of Environmental Chemical Engineering, 11*(3), 109708. doi: 10.1016/j.jece.2023.109708
38. Sun X., Guo Y., Yan Y., Li J., Shen J., Han W., et al. (2019): Co-processing of MSWI fly ash and copper smelting wastewater and the leaching behavior of the co-processing products in landfill leachate. *Waste Management, 95*, 628-635. doi: 10.1016/j.wasman.2019.07.003
39. Chen Z., Li J. S., Zhan B. J., Sharma U., Poon C. S. (2018): Compressive strength and microstructural properties of dry-mixed geopolymer pastes synthesized from GGBS and sewage sludge ash. *Construction and Building Materials, 182*, 597-607. doi: 10.1016/j.conbuildmat.2018.06.159
40. Zhan X., Kirkelund G. M. (2021): Electrodialytic remediation of municipal solid waste incineration fly ash as pre-treatment before geopolymerisation with coal fly ash. *Journal of Hazardous Materials, 412*, 125220. doi: 10.1016/j.jhazmat.2021.125220
41. Liu X., Zhao X., Yin H., Chen J., Zhang N. (2018): Intermediate-calcium based cementitious materials prepared by MSWI fly ash and other solid wastes: hydration characteristics and heavy metals solidification behavior. *Journal of Hazardous Materials, 349*, 262-271. doi: 10.1016/j.jhazmat.2017.12.072
42. Jose A., Nivitha M.R., Krishnan J.M., Robinson R.G. (2020): Characterization of cement stabilized pond ash using FTIR spectroscopy. *Construction and Building Materials, 263*, 120136. doi: 10.1016/j.conbuildmat.2020.120136
43. Peyne J., Gautron J., Doudeau J., Joussein E., Rossignol S. (2017): Influence of calcium addition on calcined brick clay based geopolymers: A thermal and FTIR spectroscopy study. *Construction and Building Materials, 152*, 794-803. doi: 10.1016/j.conbuildmat.2017.07.047
44. Wang S., Yu L., Qiao Z., Deng H., Xu L., et al. (2023): The toxic leaching behavior of MSWI fly ash made green and non-sintered lightweight aggregates. *Construction and Building Materials, 373*, 130809. doi: 10.1016/j.conbuildmat.2023.130809
45. Guo L., Zhao W., Guo L., Wang Z. (2023): Study on mechanical properties and pore structure characteristics of alkali activation sludge-cement composites. *Materials Today Communications, 35*, 105469. doi: 10.1016/j.mtcomm.2023.105469
46. Wang Y., Hu Y., Xue C., Khan A., Zheng X., Cai L. (2022): Risk assessment of lead and cadmium leaching from solidified/stabilized MSWI fly ash under long-term landfill simulation test. *Science of the Total Environment, 816*, 151555. doi: 10.1016/j.scitotenv.2021.151555